Pertanika J. Sci. & Technol. 25 (3): 995 - 1008 (2017)

SCIENCE & TECHNOLOGY

Journal homepage: http://www.pertanika.upm.edu.my/

Stability of water lubricated bearing using linear perturbation method under turbulent conditions

R. Mallya[1]*, B. S. Shenoy[2], R. S. Pai[2] and R. Pai[3]

[1]*Department of Mechanical Engineering, Canara Engineering College, Benjanapadavu, Karnataka 574219, India*

[2]*Department of Aeronautical and Automobile Engineering, Manipal Institute of Technology, Manipal University, Karnataka 576104, India*

[3]*Department of Mechanical and Manufacturing Engineering, Manipal Institute of Technology, Manipal University, Karnataka 576104, India*

ABSTRACT

The stability of a bearing is influenced by the turbulent conditions encountered during its operation. In this paper, a linearised perturbation method is used to theoretically investigate the stability of a three-axial groove water lubricated bearing. The stiffness and the damping coefficients are plotted for different eccentricity ratios of the bearing, for groove angles of 36° and 18°. The mass parameter and the whirl ratio, which are a measure of stability, are also plotted against the bearing number for different values of Reynolds number. The bearing shows very good stability at higher eccentricity ratios. The stiffness and damping coefficients as well as the mass parameter increase as the Reynolds number increases. The whirl ratios are unaffected by the change in Reynolds number.

Keywords: Axial groove, hydrodynamic pressure, journal bearing, stability, turbulent regime, water lubrication

INTRODUCTION

Fluid film bearings are susceptible to instability to certain extent. Litwin (2009) states that strict environmental laws, the growing awareness of environmental conservation, penalties for discharging toxic substances to the ocean, and economical estimates have resulted in enhancing the use of water-lubricated bearings. These bearings consist of a flat region called staves or lands which support the load. The flat regions are separated by axial grooves called flutes. The instability of a fluid film bearing is influenced by many

Article history:
Received: 11 January 2017
Accepted: 21 April 2017

E-mail addresses:
ravindramallya@gmail.com (R. Mallya),
satishshenoyb@yahoo.com (B. S. Shenoy),
ramamohan.pai@manipal.edu (R. S. Pai),
rbpai@yahoo.com (R. Pai)
*Corresponding Author

ISSN: 0128-7680

parameters. To prevent instability in plain cylindrical bearings, and enhance the stable speed range of the equipment designers have considered different geometries like multi-lobe, tilting pad, pressure dam, wave bearing design etc (Kakoty & Majumdar 1999). The mass of fluid is generally ignored in the study of bearing instability because of the negligible inertia effect in the calculation of the fluid film forces. The use of low viscosity fluids like water and the high-speed conditions of present day machinery make it necessary to consider the effects of fluid film inertia. The effects of turbulence and inertia of the lubricant film on bearing behavior increase as the Reynolds number increases.

The dynamic stability of a rotor supported by fluid film bearings can be studied by two different approaches, linear perturbation analysis and non-linear transient analysis. A small perturbation is assumed to be imposed on the journal centre around its equilibrium position in the linear perturbation theory. This method calculates the stiffness and damping coefficients that characterizes the equilibrium position at the shaft centre. The calculated coefficients are subsequently used to compute the critical mass and the whirl frequency. The set of stiffness and damping coefficients established, evaluates the vibration characteristics of the hydrodynamic film. The coefficients are computed from the solutions of the Reynolds equation as stated by Stachowiak and Batchelor (2013). Majumdar, Pai and Hargreaves (2004) in their analysis of water lubricated journal bearing with three axial grooves have concluded that smaller groove angle increase both load capacity and stability.

Kakoty and Majumdar (2000) in their linear perturbation analysis concluded that fluid inertia was independent of the steady state characteristics. Shenoy and Pai (2010) incorporated laminar and turbulence effects in externally adjustable fluid film bearing and observed that both in laminar as well as in turbulent flow the load capacity increases as the film thickness reduces. For a particular eccentricity value and misalignment, the shaft attitude angle and the friction value increased. Capone, Russo and Russo (1991) have theoretically analysed the influence of inertia and turbulence on the dynamic characteristics of bearings for various values of Reynolds number. From the different plots, it was observed that the direct stiffness coefficients changed their trend as the Reynolds number was varied. It was also observed that, the cross-coupled stiffness coefficients were affected by turbulence and fluid inertia. Pai, Rao, Shenoy and Pai (2012) in their study on tri taper journal bearing found the critical mass parameter increased with the increase in the ramp size to contribute to an improvement in the stability of the bearing. The variation in film thickness of the lubricant also affected the performance characteristics of the bearing. Rao and Sawicki (2002) have theoretically analyzed the effect of cavitation on fluid film bearing using linear stability analysis. Their theoretical results were in close agreement with the experimental published work. The study validated the significance of incorporating cavitation flow modelling in linear stability analysis of journal bearing. Hashimoto and Wada (1982a) in their analysis on dynamic characteristics of turbulent journal bearings observed that the whirl frequencies decreased with turbulence for all slenderness ratios, but the inertial effects were different for each slenderness ratio. The frequencies of infinitely short bearings became higher with the inertia forces at high eccentricities and decreased with changes in the slenderness ratio. Kumar and Mishra (1996) used Constantinescu's turbulent lubrication theory to investigate the stability of hydrodynamic worn journal bearings in turbulent conditions. It was observed that stability decreases initially with the wear depth parameter and then improves

when the wear depth parameter is increased. With an increase in L/D ratio, the stability of the worn bearings deteriorates when operating in turbulent lubrication regime. Worn bearings with lower L/D ratios were relatively more stable. The dynamic characteristics in journal bearing incorporating turbulence and inertia effects were studied by Hashimoto and Wada (1982b). It was found that the Sommerfeld number decreased by turbulence effects and the attitude angles increased by inertia effects. Lahmar (2005) has theoretically investigated the double-layered journal bearings lubricated with couple-stress fluids and discussed the combined effects of flow and fluid– solid interaction on the stability of double-layered journal bearings. It was observed that the peak pressure, the load capacity, stability region of the bearing increased with the couple stress parameter. In the present study, the dynamic coefficients for 3 axial water lubricated bearing in the turbulent regime are computed using the linearized bearing reaction method for groove angles 18^o and 36^o. The whirl ratio and mass parameter are also plotted for different values of bearing number for different eccentricity ratios.

METHODS

Procedure

Dynamic characteristics. The Reynolds equation governs the pressure distribution in the clearance space between journal and bearing. To study the turbulent flow in a fluid film, the Reynolds equation is modified by introducing 'turbulence coefficients'. The equation [1] shows the modified Reynolds equation.

$$\frac{\partial}{\partial x}\left[\frac{1}{k_\theta}h^3\frac{\partial p^*}{\partial x}\right]+\frac{\partial}{\partial z}\left[\frac{1}{k_z}h^3\frac{\partial p^*}{\partial \theta}\right]=\frac{1}{2}U\eta\frac{\partial h}{\partial x}+\eta\frac{\partial h}{\partial t} \quad [1]$$

The governing equation [1] in non-dimensional form, reduces to

$$\frac{1}{k_\theta}\left[\frac{\partial}{\partial\theta}\left(\left(\overline{h}^3\right)\frac{\partial\overline{p}}{\partial\theta}\right)\right]+\frac{1}{k_z}\left(\frac{R^2}{L^2}\right)\left[\frac{\partial}{\partial\overline{z}}\left(\left(\overline{h}^3\right)\frac{\partial\overline{p}}{\partial\overline{z}}\right)\right]=\frac{1}{2}\frac{\partial\overline{h}}{\partial\theta} \quad [2]$$

The turbulence model used is Ng – Pan where the coefficients k_θ and k_z are calculated as

$$k_\theta = 12 + k_x(Re_L)^{n_x} \quad [3]$$

$$k_z = 12 + k_{zz}(Re_L)^{n_z} \quad [4]$$

The values for k_x, n_x, k_{zz} and n_z are listed in the table 1 as suggested by Taylor & Dowson (1974).

Table 1
Turbulence parameters from Taylor and Dowson (1974)

	k_x	n_x	k_{zz}	n_z
$Re_L \geq 50{,}000$	0.0388	0.80	0.0213	0.80
$10{,}000 \leq Re_L < 50{,}000$	0.0250	0.84	0.0136	0.84
$5{,}000 \leq Re_L < 10{,}000$	0.0250	0.84	0.0088	0.88
$Re_L < 5{,}000$	0.0039	1.06	0.0021	1.06

The boundary conditions used are the Reynolds boundary conditions, i.e. $\overline{p} = 0$, when $\frac{\partial \overline{p}}{\partial \theta} = 0$. It is assumed that journal moves in a periodic movement with small amplitude of $Re(C\varepsilon_1 e^{i\tau})$ along the line of centres and $Re(C\varepsilon_0 \phi_1 e^{i\tau})$ perpendicular to the line of centres. The journal moves around its steady state position of ε_o and ϕ_o. When the instability of the journal begins, the initial position of the journal centre can be termed as a steady state value (ε_o, ϕ_o) together with a harmonic vibration of frequency ω_p thus

$$\varepsilon = \varepsilon_o + \varepsilon_1 e^{i\tau}, \; \phi = \phi_o + \phi_1 e^{i\tau}$$

Where, $|\varepsilon_1| \ll \varepsilon_0$, $|\phi_1| \ll \phi_0$.

When the journal is functioning under very small amplitude of vibration, first order perturbation method will be applicable. The pressure and film thickness equations are written as

$$\overline{p} = \overline{p}_o + \varepsilon_1 e^{i\tau} \overline{p}_1 + \varepsilon_o \phi_1 e^{i\tau} \overline{p}_2 \qquad [5]$$

$$\overline{h} = \overline{h}_o + \varepsilon_1 e^{i\tau} \cos\theta + \varepsilon_o \phi_1 e^{i\tau} \sin\theta \qquad [6]$$

Substitution of equation [5] and [6] in equation [2] and holding on to first linear terms will result in the equations [7], [8] and [9].

$$\varepsilon_o \qquad \frac{12}{k_\theta}\left[\overline{h}_o^{\,3} \frac{\partial^2 \overline{p}_o}{\partial \theta^2} + 3\overline{h}_o^{\,2} \frac{\partial \overline{h}_o}{\partial \theta} \frac{\partial \overline{p}_o}{\partial \theta}\right] + \frac{12}{k_z}\left(\frac{R}{L}\right)^2 \overline{h}_o^{\,3} \frac{\partial^2 \overline{p}_o}{\partial \overline{z}^2} - \Lambda \frac{\partial \overline{h}_o}{\partial \theta} - 2\lambda\Lambda \frac{\partial \overline{h}_o}{\partial \tau} = 0 \qquad [7]$$

$$\varepsilon_1 e^{i\tau} \qquad \frac{12}{k_\theta}\left[\begin{array}{l} \overline{h}_o^{\,3} \frac{\partial^2 \overline{p}_1}{\partial \theta^2} + 3\overline{h}_o^{\,2} \cos\theta \frac{\partial \overline{h}_o}{\partial \theta} \frac{\partial^2 \overline{p}_o}{\partial \theta^2} - 3\overline{h}_o^{\,2} \sin\theta \frac{\partial \overline{p}_o}{\partial \theta} + \\ 6\overline{h}_o \frac{\partial \overline{h}_o}{\partial \theta} \frac{\partial \overline{p}_o}{\partial \theta} \cos\theta + 3\overline{h}_o^{\,2} \frac{\partial \overline{h}_o}{\partial \theta} \frac{\partial \overline{p}_1}{\partial \theta} \end{array}\right] + \frac{12}{k_z}\left(\frac{R}{L}\right)^2 \left[\overline{h}_o^{\,3} \frac{\partial^2 \overline{p}_1}{\partial \overline{z}^2} + 3\overline{h}_o^{\,2} \cos\theta \frac{\partial^2 \overline{p}_o}{\partial \overline{z}^2}\right]$$

$$+ \Lambda \sin\theta - 2i\Lambda\lambda \cos\theta = 0 \qquad [8]$$

$$\varepsilon_o \phi_1^{\,i\tau} \quad \frac{12}{k_\theta}\left[\begin{array}{l}\bar{h}_o^{\,3}\frac{\partial^2 \bar{p}_2}{\partial\theta^2}+3\bar{h}_o^{\,2}\sin\theta\frac{\partial^2 \bar{p}_o}{\partial\theta^2}+3\bar{h}_o^{\,2}\cos\theta\frac{\partial \bar{p}_o}{\partial\theta}+\\ 6\bar{h}_o\frac{\partial \bar{h}_o}{\partial\theta}\frac{\partial \bar{p}_o}{\partial\theta}\sin\theta+3\bar{h}_o^{\,2}\frac{\partial \bar{h}_o}{\partial\theta}\frac{\partial \bar{p}_2}{\partial\theta}\end{array}\right]+\frac{12}{k_z}\left(\frac{R}{L}\right)^2\left[\bar{h}_o^{\,3}\frac{\partial^2 \bar{p}_2}{\partial\bar{z}^2}+3\bar{h}_o^{\,2}\sin\theta\frac{\partial^2 \bar{p}_o}{\partial\bar{z}^2}\right]$$

$$+\Lambda\cos\theta-2i\Lambda\lambda\sin\theta=0 \qquad [9]$$

The dynamic movement of the centre of the journal, $Re(C\varepsilon_1 e^{i\tau})$ being in the parallel and $Re(C\varepsilon_0\phi_1 e^{i\tau})$ in the perpendicular direction of the line of centres will be used to compute the dynamic pressures $\bar{p}_1$ and $\bar{p}_2$. The load components of the dynamic pressures along and at right angles to the line of centres are mentioned in equations [10] and [11].

$$(W_1)_r=\int_0^L\int_0^{2\pi} p_1 R\cos\theta\, d\theta\, dz \qquad [10]$$

$$(W_1)_\phi=\int_0^L\int_0^{2\pi} p_1 R\sin\theta\, d\theta\, dz \qquad [11]$$

The equations [12] to [15] are used to compute the stiffness and the damping values of the journal bearing

$$\bar{K}_{rr}=-Re\left(\int_0^1\int_0^{2\pi}\bar{p}_1\cos\theta\, d\theta\, d\bar{z}\right) \qquad [12]$$

$$\bar{K}_{\phi r}=-Re\left(\int_0^1\int_0^{2\pi}\bar{p}_1\sin\theta\, d\theta\, d\bar{z}\right) \qquad [13]$$

$$\bar{D}_{rr}=-Im\left(\frac{\int_0^1\int_0^{2\pi}\bar{p}_1\cos\theta\, d\theta\, d\bar{z}}{\lambda}\right) \qquad [14]$$

$$\bar{D}_{\phi r}=-Im\left(\frac{\int_0^1\int_0^{2\pi}\bar{p}_1\sin\theta\, d\theta\, d\bar{z}}{\lambda}\right) \qquad [15]$$

Where $\bar{K}_{ij}=\dfrac{K_{ij}C}{LDp_s}$ and $\bar{D}_{ij}=\dfrac{D_{ij}C\omega}{LDp_s}$

Similarly, equations [16] to [19] give the stiffness and damping values considering the dynamic movement of the centre of the shaft along the ϕ direction,

$$\overline{K}_{\phi\phi} = -Re\left(\int_0^1\int_0^{2\pi} \overline{p}_2 \sin\theta \, d\theta \, d\bar{z}\right) \quad [16]$$

$$\overline{K}_{r\phi} = -Re\left(\int_0^1\int_0^{2\pi} \overline{p}_2 \cos\theta \, d\theta \, d\bar{z}\right) \quad [17]$$

$$\overline{D}_{\phi\phi} = -Im\left(\frac{\int_0^1\int_0^{2\pi} \overline{p}_2 \sin\theta \, d\theta \, d\bar{z}}{\lambda}\right) \quad [18]$$

$$\overline{D}_{r\phi} = -Im\left(\frac{\int_0^1\int_0^{2\pi} \overline{p}_2 \cos\theta \, d\theta \, d\bar{z}}{\lambda}\right) \quad [19]$$

Stability criteria. The rotor is assumed to be stiff or inelastic and considered to have mass M. The stability of the rotating journal is evaluated by computing the film forces F_r and F_ϕ, which is obtained by combining the equations of motion [20] and [21].

$$F_r + W\cos\phi - MC\left[\frac{d^2\varepsilon}{dt^2} - \varepsilon\left(\frac{d\phi}{dt}\right)^2\right] = 0 \quad [20]$$

$$F_\phi - W\sin\phi - MC\left[\varepsilon\frac{d^2\phi}{dt^2} + 2\frac{d\varepsilon}{dt}\frac{d\phi}{dt}\right] = 0 \quad [21]$$

After substituting ε, ϕ and non-dimensionalising and simplifying,

$$\overline{M} = \frac{1}{\lambda^2\left(\overline{D}_{\phi\phi} + \overline{D}_{rr}\right)}\left[\begin{array}{l}\left(\overline{D}_{rr}\overline{K}_{\phi\phi} + \overline{K}_{rr}\overline{D}_{\phi\phi}\right) - \left(\overline{K}_{\phi r}\overline{D}_{r\phi} + \overline{D}_{\phi r}\overline{K}_{r\phi}\right) \\ + \dfrac{\overline{W}}{\varepsilon_o}\left(\overline{D}_{rr}\cos\phi_o - \overline{D}_{\phi r}\sin\phi_o\right)\end{array}\right] \quad [22]$$

$$\overline{M}^2\lambda^4 - \lambda^2\left[\overline{M}\left(\frac{\overline{W}\cos\phi_o}{\varepsilon_o} + \overline{K}_{\phi\phi} + \overline{K}_{rr}\right) + \left(\overline{D}_{rr}\overline{D}_{\phi\phi} - \overline{D}_{\phi r}\overline{D}_{r\phi}\right)\right]$$
$$+\left(\overline{K}_{rr}\overline{K}_{\phi\phi} - \overline{K}_{\phi r}\overline{K}_{r\phi}\right) + \frac{\overline{W}}{\varepsilon_o}\left(\overline{K}_{rr}\cos\phi_o - \overline{K}_{\phi r}\sin\phi_o\right) = 0 \quad [23]$$

Equations [22] and [23] use the computed stiffness and damping coefficients to evaluate the stability of a rigid journal held by the bearing. $\overline{M}$ and λ are the solutions calculated from equations [22] and [23] which are linear algebraic equations. The threshold speed of journal is calculated from this value of $\overline{M}$. The bearing system will be unstable if the speed of the system goes beyond the limiting speed. The rotating speed of the shaft centre can be found from the whirl ratio. The rotation of the shaft and the rotation of its centre are in the same direction.

Solution Procedure

The solution method used here is similar to that of Majumdar et al. (2004). A second-order finite difference method was used for solving the governing Reynolds equation incorporated with the turbulent coefficients. A programmable code in MATLAB R2012b was written to calculate the non-dimensional dynamic pressure. The circumferential coordinate θ for an axial groove bearing is considered from the region of maximum film thickness. Initially, an arbitrary value of attitude angle is considered, the solution converges when the arbitrary value and the calculated value of attitude angle for a given accuracy is achieved. The calculated attitude angle is considered by the program to compute the dynamic non – dimensional pressure. The aspect ratio of the grid was kept equal; increment in θ direction $\delta\theta$, and increment in the z direction δz, both were kept equal to 0.0524. The iterative procedure of calculation with an accuracy value of 0.0001 at the nodes was used for the convergence of the pressure. A relaxation factor of 1.3 was implemented to accelerate the convergence of dynamic pressure. The dynamic loads are calculated using the equations [10] and [11]. The program computes both the stiffness and damping coefficients, given in the equations [12] to [19]. The stability criterion of the bearing is analysed using equations [22] and [23] where the mass parameter and the whirl ratio are calculated. The L/D value is taken as 1 for both the groove angles.

Validation

Figure 1 and 2 show the validation of the codes used. The results of the codes are validated with the published data from Majumdar et al. (2004). The plots from the present analysis in the Figure 1 are of critical mass parameter and whirl ratio considering the flow of the lubricant in the laminar regime. The nature of the plots in Figure 1 and Figure 2 are in good agreement, with little variation in the values.

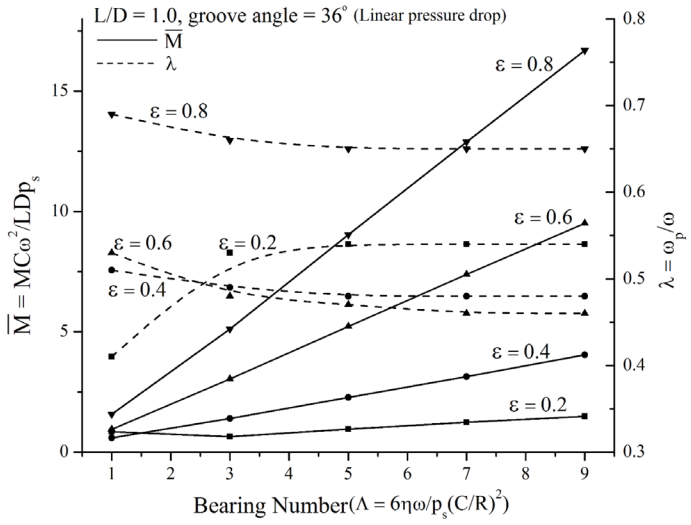

Figure 1. Effect of Critical Mass variable $(\overline{M})$ and whirl ratio (λ) with bearing no. for different eccentricity ratios (Present analysis)

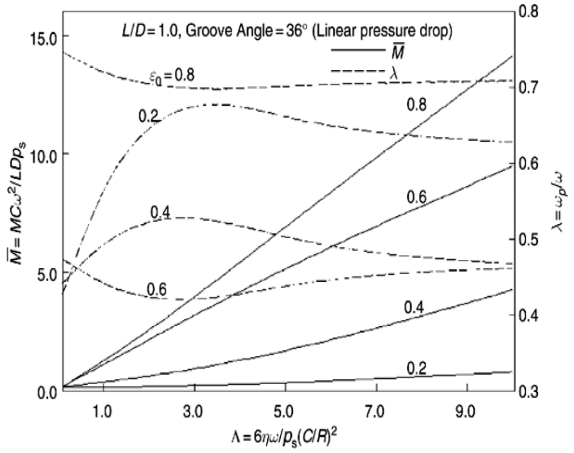

Figure 2. Effect of Mass variable $(\overline{M})$ & whirl ratio (λ) with various bearing no. for different eccentricity ratios, from Majumdar et al. (2004)

RESULTS AND DISCUSSIONS

Figure 3, 4 and 5 are the graphs for mass parameter versus bearing number for different values of eccentricity ratios. The whirl ratio versus bearing number is also plotted in the same graph. The groove angle considered is 18° with values of Re varying from 4000 to 55,000. Figure 6, 7 and 8 are the similar plots for groove angle 36°. The major factors responsible for whirl instability are the two coefficients calculated from the codes, stiffness coefficients $\overline{K}_{ij}$ and damping coefficients $\overline{D}_{ij}$. The individual coefficients of either stiffness or damping do not indicate stability characteristics. The computed coefficient values are substituted in the equations of motion to obtain threshold or limiting speed of the bearing. The threshold speed

is the limiting speed within which the bearing has to operate. The bearing becomes unstable if the speed of the bearing goes beyond the threshold speed. The value of mass parameter, $\overline{M}$ gives the threshold speed. The whirl speed is established from the whirl ratio λ for a given journal speed. $\overline{M}$ and λ, are the factors used to quantify the stability of the bearing. The upper region of the curve in all the figures 3 to 8 of $\overline{M}$ versus bearing number are unstable. The journal bearing system should function within the stable region. The stable region of the bearing increases as the eccentricity ratio is increased. The axial groove journal bearings, irrespective of the turbulent conditions and groove angles, show higher values of $\overline{M}$, thereby revealing that; theoretically, the bearings become stable when they are operating in high eccentricities. It can also be observed that for the same value of Reynolds number, the $\overline{M}$ value for the bearing with the 18° groove angle is more than that for 36° groove angle. This indicates that a bearing having smaller groove angle is more stable than that with a higher groove angle. The stability of the bearing improved with the increase in the Reynolds number and increase in eccentricity ratio as seen from all the plots. The values of the whirl ratios reduce when the bearing is operating in the higher eccentricity as seen from all the graphs. The value of λ decreases for both the groove angles for $\varepsilon = 0.8$ and $\varepsilon = 0.6$. Theoretically, the influence of turbulent flow affects the stability of the bearing as seen from all the plots.

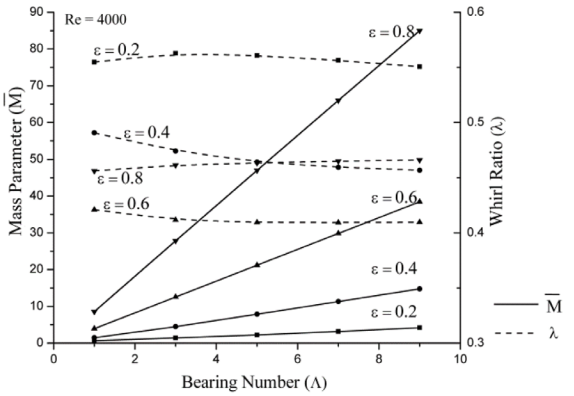

Figure 3. Effect of Reynolds Number (Re = 4000) on Mass variable, whirl ratio with various bearing no. for various ε for groove angle 18°

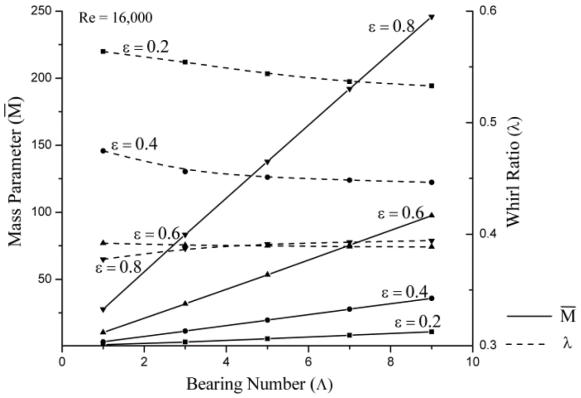

Figure 4. Effect of Reynolds Number (Re = 16,000) on Mass variable, whirl ratio with various bearing no. for various ε for groove angle 18°

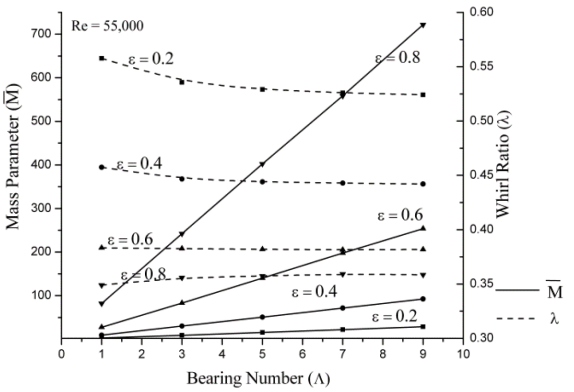

Figure 5. Effect of Reynolds Number (Re = 55,000) on Mass variable, whirl ratio with various bearing no. for various ε for groove angle 18°

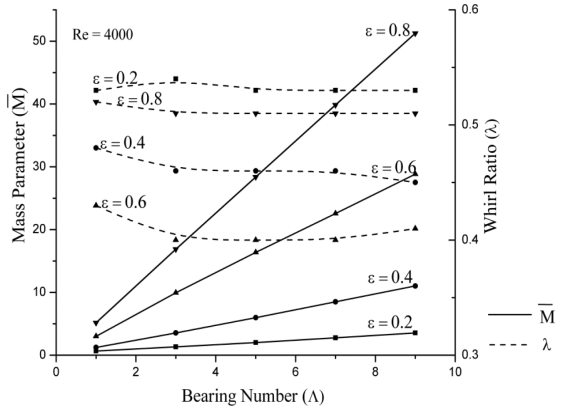

Figure 6. Effect of Reynolds Number (Re = 4000) on Mass variable, whirl ratio with various bearing no. for various ε for groove angle 36°

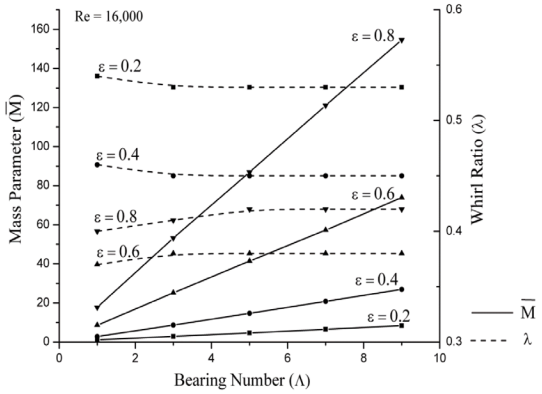

Figure 7. Effect of Reynolds Number (Re = 16,000) on Mass variable, whirl ratio with various bearing no. for various ε for groove angle 36°

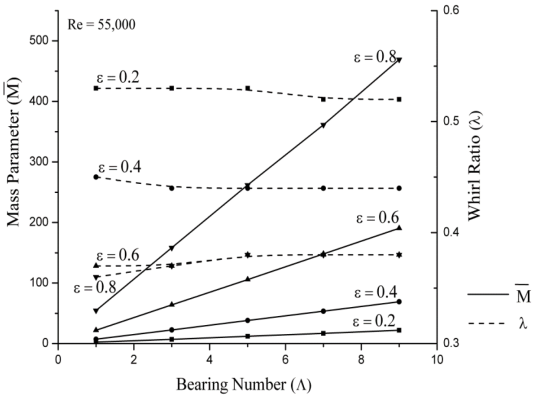

Figure 8. Effect of Reynolds Number (Re = 55,000) on Mass variable, whirl ratio with various bearing no. for various ε for groove angle 36°

CONCLUSIONS

It can be concluded that turbulence can affect the stability of the bearing. As the Reynolds number increases, it is seen that the stability region for the bearing improves. Irrespective of the groove angle and the Reynolds number at which the bearing is operating there is no significant changes in the whirl ratio for the range of eccentricity ratios considered. The groove angles considered do not result in a large variation of the calculated Mass parameter for the various Reynolds numbers at which the analysis has been performed.

REFERENCES

Cabrera, D. L., Woolley, N. H., Allanson, D. R., & Tridimas, Y. D. (2005). Film pressure distribution in water-lubricated rubber journal bearings. *Proceedings of the Institution of Mechanical Engineers, Part J: Journal of Engineering Tribology, 219*(2), 125-132. doi: 10.1243/135065005X9754

Capone, G., Russo, M., & Russo, R. (1991). Inertia and turbulence effects on dynamic characteristics and stability of rotor-bearings systems. *Journal of Tribology, 113*(1), 58-64. doi:10.1115/1.2920604

Hashimoto, H., & Wada, S. (1982a). An analysis of dynamic characteristics of turbulent journal bearings considering inertia forces. *Bulletin of JSME, 25*(208)*,* 208-15. Retrieved from http://doi.org/10.1299/jsme1958.25.1601

Hashimoto, H., & Wada, S. (1982b). An influence of inertia forces on the stability of turbulent journal bearings. *Bulletin of JSME, 25*(202), 202-223. doi:10.1299/jsme1958.25.653

Kakoty, S. K., & Majumdar, B. C. (1999). Effect of fluid inertia on stability of flexibly supported oil journal bearings: linear perturbation analysis. *Tribology International, 32*(4), 217-228. doi:10.1016/S0301-679X (99)00036-5

Kakoty, S. K., & Majumdar, B. C. (2000). Effect of fluid inertia on the dynamic coefficients and stability of journal bearings. *Proceedings of the Institution of Mechanical Engineers, Part J: Journal of Engineering Tribology,* 214(3), 229-240. doi:10.1243/1350650001543133

Kumar, A., & Mishra, S. S. (1996). Stability of a rigid rotor in turbulent hydrodynamic worn journal bearings. *Wear, 193*(1), 25-30. doi:10.1016/0043-1648(95)06654-3

Lahmar, M. (2005). Elastohydrodynamic analysis of double-layered journal bearings lubricated with couple-stress fluids. *Proceedings of the Institution of Mechanical Engineers, Part J: Journal of Engineering Tribology, 219*(2), 145-165. doi:10.1243/135065005X9835

Litwin, W. (2009). Water lubricated bearings of ship propeller shafts– problems, experimental tests and theoretical investigations. *Polish Maritime Research, 16*(4), 42-50. doi: 10.2478/v10012-008-0055-z

Majumdar, B. C., Pai, R., & Hargreaves, D. J. (2004). Analysis of water-lubricated journal bearings with multiple axial grooves. *Proceedings of the Institution of Mechanical Engineers, Part J: Journal of Engineering Tribology, 218*(2), 135-146. doi: 10.1177/135065010421800208

Pai, R., Rao, D. S., Shenoy, B. S., & Pai, R. S. (2012). Stability characteristics of a tri–taper journal bearing: A linearized perturbation approach. *Journal of Materials Research and Technology, 1*(2), 84-90. doi: 10.1016/S2238-7854(12)70016-9

Rao, T. V. V. L. N., & Sawicki, J. T. (2002). Linear stability analysis for a hydrodynamic journal bearing considering cavitation effects. *Tribology Transactions, 45*(4), 450-456. doi:10.1115/1.1828451

Shenoy, B. S., & Pai, R. (2010). Stability characteristics of an externally adjustable fluid film bearing in the laminar and turbulent regimes. *Tribology International, 43*(9), 1751-1759. doi:10.1016/j.triboint.2010.04.015

Stachowiak, G., & Batchelor, A. W. (2013). *Engineering Tribology*. United States of America, USA: Butterworth-Heinemann

Taylor, C. M., & Dowson, D. (1974). Turbulent lubrication theory – application to design. *Journal of Lubrication Technology, 96*(1), 36-47. doi:10.1115/1.3451905

NOMENCLATURE

C Clearance between shaft and bearing (m)

D Bearing Diameter (m)

$D_{rr}, D_{\phi\phi}, D_{\phi r}, D_{r\phi}$ Damping coefficient (Ns/m)

$\overline{D}_{rr}, \overline{D}_{\phi\phi}, \overline{D}_{\phi r}, \overline{D}_{r\phi}$ Non dimensional damping coefficient, $\overline{D}_{i,j} = D_{i,j} C\omega / LDp_s$

F_r Dynamic force of lubricant film along the radial direction (N)

F_ϕ Dynamic force of lubricant film along ϕ the direction (N)

h, $\overline{h}$ film thickness (m), $\overline{h} = h / C$

$K_{rr}, K_{\phi\phi}, K_{\phi r}, K_{r\phi}$ Stiffness coefficient (N/m)

$\overline{K}_{rr}, \overline{K}_{\phi\phi}, \overline{K}_{\phi r}, \overline{K}_{r\phi}$ Non dimensional stiffness coefficient $\overline{K}_{i,j} = K_{i,j} C / LDp_s$

M, $\overline{M}$ Mass of the Rotor (kg), mass variable $\overline{M} = \dfrac{MC\omega^2}{LDP_s}$

p, $\overline{p}$ Lubricant film pressure (Pa), $\overline{p} = pC^2 / \eta UR$, $\overline{p} = p / p_s$

p_s Lubricant supply pressure (Pa)

$\overline{p}_1, \overline{p}_2$ Perturbed pressure

R Journal radius (m)

Re Global Reynolds Number

x Coordinates in circumferential direction

U Journal velocity = ωR (m/s)

W Load during steady state (N)

W_r, W_t Load components along and perpendicular to the line joining the centres respectively (N)

z Axial direction coordinate axis (m)

ε Eccentricity Ratio = e/C

ε_1, ϕ_1 Perturbation parameters

η Absolute viscosity coefficient (Pa-s)

$\theta, \bar{z}$ Non dimensional coordinates measured from the line joining the centers, $\theta = x / R,\ \bar{z} = z / L$

θ^* Circumferential coordinate measured from the centre of the groove

λ Whirl ratio = ω / ω_p

Λ Bearing number = $6\eta\omega / \left[p_s (C/R)^2\right]$

τ Non-dimensional time, $\omega_p t$

ϕ Attitude angle (rad)

ω Rotation speed of journal (rad/s)

ω_p Journal vibration frequency (rad/s)

$(\ )_o$ Steady state value